CFD analysis of the transient flow in a low-oil concentration hydrocyclone

Paladino, E. E.[(1)], Nunes, G. C. [(2)] and Schwenk, L.[(1)]

(1) ESSS – Engineering Simulation and Scientific Software – CELTA - Rod SC-401, Km001 - Florianopolis - SC – Brazil. CEP: 88030-000
(2) CENPES – PETROBRAS Research and Development Center - Cidade Universitaria Q.7 - Ilha do Fundão - Rio de Janeiro - RJ - Brazil. CEP: 21949-900

Prepared for Presentation at AIChE 2005 Annual Meeting, October 30 - November 4, Cincinnati, Ohio, at: Poster Session in Fluid Mechanics (01J11)

Unpublished

ABSTRACT

This work presents a CFD analysis in a DE-OILER hydrocyclone. This device is used to separate the residual oil (of order of 1000 ppm's) present in the water produced from the oil wells, after primary oil separation. The aim of the work is to develop a CFD model to analyze the flow pattern, pressure drop and separation efficiency of the hydrocyclone. One of the goals of the project is to run a CFD model for different operational conditions and use the results to design a control loop for the hydrocyclone operation. In addition, within this context, the transient behavior was analyzed in order to evaluate the characteristic times of the device, *i.e.*, evaluate the necessary time to stabilize the hydrocyclone operation under changes in operational conditions. The SSG (Speziale, Sarkar, and Gatski (1991)) Reynolds Stress Model was used to compute the effects of turbulence, which uses a quadratic relation for the pressure-strain correlation and is known to properly predict the characteristic reverse flow in these devices. The Algebraic Slip Model was used to evaluate the separation efficiency. This approach for the dispersed oil flow allowed considering a size distribution for the oil droplets at low computational cost.

Key words: numerical simulation, algebraic slip (drift flux) model, hydrocyclone, oil-water separation

Introduction

This work describes the development of a CFD model to study the two-phase flow behavior within an oil/water separation hydrocyclone, including its transient behavior under changes in operational conditions. One important objective of the project is to develop a control loop for the hydrocyclone operation. Then, the CFD model will be used to obtain operating curves of the device by running the model several times for different operating conditions. After that, these curves will be used to design and implement the control loop for the device.

According to this objective, an interesting point investigated was the transient behavior of the hydrocyclone when operational conditions are suddenly changed. The idea was to use the CFD model to estimate the needed time in order the system stabilize its operation and reach a steady state condition. This is also important to verify validity of the hypothesis of considering the changes in the operational condition as a sequence of steady states. If this time is small when compared with the characteristic times of the control loop (like the time necessary to open or close a valve) the dynamic behavior of the flow can be considered independent from the control loop implementation.

Another objective of the model was to study the hydrocyclone separation efficiency. For this purpose the ASM (Algebraic Slip Model) (Ishii (1977); Manninen & Tavassalo (1996)) was implemented and used to estimate this parameter.

The following sections presents the details of the mathematical and computational model implemented and the results obtained for both models.

Mathematical modeling

This section describes the mathematical model used to compute the flow inside the hydrocyclone. Some characteristics of the turbulence model will be pointed out and then, the ASM model used to include the oil phase will be described.

The mass and momentum conservation equations are given by,

$$\frac{\partial}{\partial t}(\rho) + \nabla \cdot (\rho \mathbf{U}) = 0 \qquad \textbf{(1)}$$

$$\frac{\partial}{\partial t}(\rho \mathbf{U}) + \nabla \cdot (\rho \mathbf{U}\mathbf{U}) = -\nabla p + \nabla \cdot \left(\mathbf{T} + \mathbf{T}^{Turb}\right) + \rho \mathbf{f} \qquad \textbf{(2)}$$

Where $\mathbf{T}^{Turb}$ represents the turbulent stress tensor. For the flow calculation within cyclones, it is commonly recommended in literature, that Reynolds stress turbulence models be used. These models are capable to represent more adequately the reverse flow in the central core as they captures the characteristic non iso-tropic turbulence fluctuations of these devices. This is necessary to accurately calculate the separation efficiency. This model calculates each component of the Reynolds stress transport using a transport equation for each Reynolds Stress Tensor component like,

$$\frac{\partial}{\partial t}\left(\rho\overline{u_i u_j}\right)+\nabla\cdot\left(\rho\,\mathbf{U}\,\overline{u_i u_j}\right)=P_{ij}+\phi_{ij}+\nabla\cdot\left(\left(\mu+\frac{2}{3}C_S\rho\frac{k^2}{\varepsilon}\right)\nabla\overline{u_i u_j}\right)-\frac{2}{3}\delta_{ij}\rho\varepsilon \quad \textbf{(3)}$$

and an equation for the dissipation rate,

$$\frac{\partial}{\partial t}\left(\rho\varepsilon\right)+\nabla\cdot\left(\rho\,\mathbf{U}\,\varepsilon\right)=\frac{\varepsilon}{k}\left(C_{\varepsilon 1}P-C_{\varepsilon 2}\rho\varepsilon\right)+\nabla\cdot\left(\left(\mu+\frac{\mu_t}{\sigma_\varepsilon}\right)\nabla\varepsilon\right)-\frac{2}{3}\delta_{ij}\rho\varepsilon \quad \textbf{(4)}$$

An important term in Reynolds stress models is the pressure-strain correlation, ϕ_{ij} . This term could be expressed in a general form as:

$$\begin{aligned}\phi_{ij} = &-\rho\varepsilon\left(C_{S1}a+C_{S2}\left(aa--\frac{1}{3}a\cdot a\,\delta\right)\right)-\\ &-C_{r1}Pa+C_{r2}\rho kS-C_{r3}\rho kS\sqrt{a\cdot a}\\ &+C_{r4}\rho k\left(aS^T+Sa^T-\frac{2}{3}a\cdot S\,\delta\right)\\ &+C_{r5}\rho k\left(aW^T+Wa^T\right)\end{aligned} \quad \textbf{(5)}$$

Different alternatives have been presented in literature for the modeling of ϕ_{ij}. This work follows the Speziale, Sarkar and Gatski (Speziale *et al.* (1991)) (SSG) model which considers a quadratic relation for the pressure strain relation. This is done by considering the coefficients C_{Si} and C_{ri} non zero maintaining the quadratic relation between ϕ_{ij} and the anisotropy tensor *a*, given by,

$$a=\frac{\mathbf{u}\otimes\mathbf{u}}{k}-\frac{2}{3}\delta \quad \textbf{(6)}$$

Other approaches like that used by Launder, Reece and Rodi (Launder *et al.* (1975)) (LRR-QI and LRR-IP models) make the coefficients C_{r3} and C_{S2} equal to zero resulting in a linear relation between pressure and the anisotropy tensor.

The SSG model has shown to capture more accurately the reverse flow effects near the walls of the cyclone, compared to linear pressure-strain correlation models such as LRR.

Transient model set-up

As previously mentioned, the transient simulation intends to verify the hypothesis that the dynamic flow behavior of the hydrocyclone could be considered as a sequence of steady states within the scope of the control loop design. In order to investigate the dynamic flow behavior a sudden valve closing was imposed at hydrocyclone overflow and calculations was performed until the equilibrium was reached. The “equilibrium” was considered when pressure at inlets and outlets was stabilized (within a certain fluctuation amplitude) and mass and momentum global balances were achieved.

Steady state results previously obtained were used as initial conditions. The valve closing, was simulated as a sudden increase in a discharge coefficient at overflow. In order to simplify the modeling, this coefficient was non-dimensionalized as,

$$C_D = \frac{\dot{m}_{overf}^{current}}{\Delta p_{overf}^{current}} \Big/ \frac{\dot{m}_{overf}^{final}}{\Delta p_{overf}^{final}} \quad \textbf{(7)}$$

Then the variation of the discharge coefficient was represented as a variation of the average pressure at overflow, from the current value to the half of it.

Figure 1 shows the discharge coefficient at overflow, varying with time.

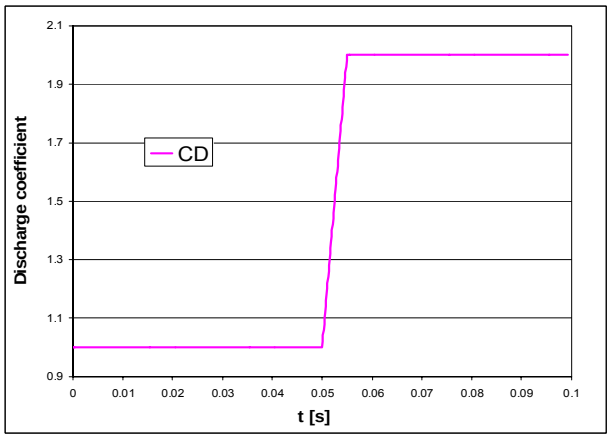

Figure 1 – Non-dimensional discharge coefficient at overflow

The ASM Model

The Algebraic Slip Model (ASM) is a simplification of the Eulerian approach used for multiphase flow, under the hypothesis that the dispersed phase instantaneously reaches the terminal velocity. This means that the relaxation time of particles is very small. This is true when relative density between phases and the disperse phase diameters are small.

The flow of both phases is solved using "bulk" transport equations, *i.e.*, the mass and momentum conservation equations for the multiphase mixture. After that, the relative velocities of the dispersed phases are solved using an algebraic equation. Two "relative" velocities are defined for the dispersed phase. The velocity relative to the mass center of the mixture (**Drift velocity**) and the velocity relative to the continuous phase (**Slip Velocity**).

So, the Slip velocity is given by,

$$\mathbf{u}_{S\alpha} = \mathbf{u}_{\alpha} - \mathbf{u}_{C} \quad \textbf{(8)}$$

And the drift velocity is,

$$\mathbf{u}_{D\alpha} = \mathbf{u}_{\alpha} - \mathbf{u}_{m} \quad \textbf{(9)}$$

These velocities are related by,

$$\mathbf{u}_{D\alpha} = \mathbf{u}_{S\alpha} - \sum_{\alpha} Y_{\alpha} \mathbf{u}_{S\alpha} \quad \textbf{(10)}$$

where Y_{α} are the mass fractions of the dispersed phases.

The slip velocities for the dispersed phases could be calculated by the relation,

$$\left|\mathbf{u}_{S\alpha}\right|\mathbf{u}_{S\alpha} = \frac{4}{3}\frac{d_p}{\rho_C C_D}\left(\rho_\alpha - \rho_m\right)\left(\frac{\partial \mathbf{u}_m}{\partial t} + \mathbf{u}_m \bullet \nabla \mathbf{u}_m - g\right) \qquad (11)$$

Details of the deduction of this equation could be found in Ishii (1977) or CFX10 Solver Theory Manual.

CFD model and boundary conditions

As described in previous sections, the Reynolds Stress Model (RSM) was used to include the turbulence effects in the continuous (water) phase. The oil phase flow was simulated through the Algebraic Slip Model, because of the very low volume fraction (of order of 0.1%) similar fluid densities (oil-water) and small droplet size.

One of the advantages of the ASM is that, due to its simplicity, several drop sizes could be run at a reasonable computational cost. In this case, the oil droplet size distribution was represented by six droplet size groups obtained by dividing the measured values in six groups and summing the corresponding volume fractions. Figure 2 shows the measured oil droplets size distribution for the inlet stream and, on the right, is showed the size distribution used in the computational model, represented by six size groups.

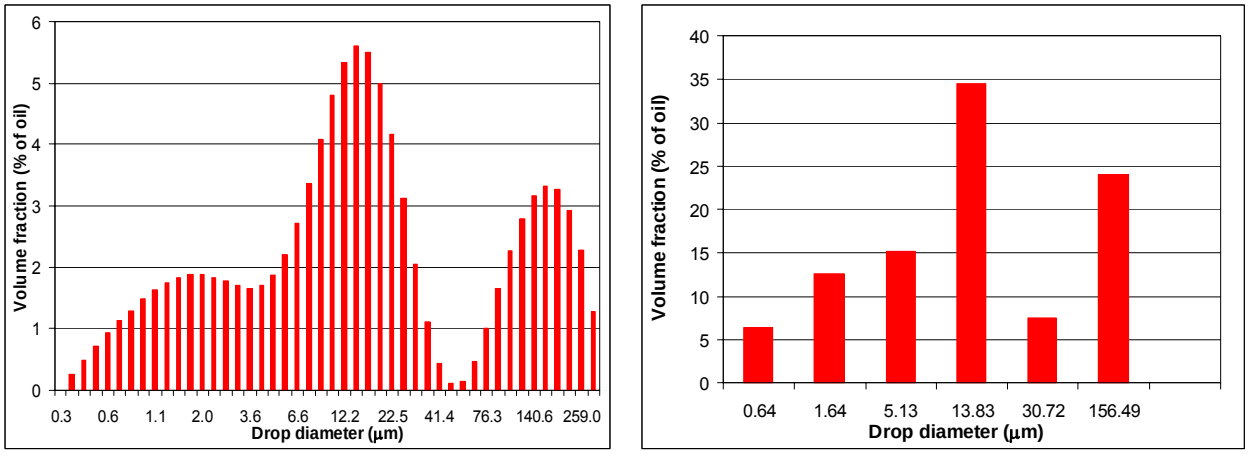

Actual measured distribution **Computational model distribution**

Figure 2 – Oil droplets size distribution at inlets.

Figure 3 shows the computational grid used to perform the simulations. ICEMCFD HEXA software was used for grid generation. Grid refinement at wall region and central core was used in order to capture the high velocity gradients at these regions.

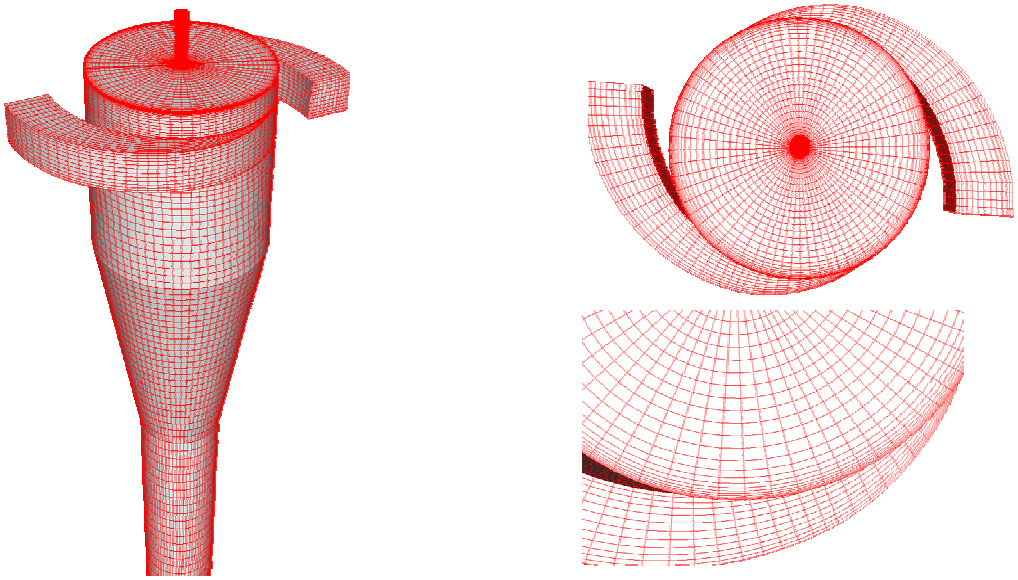

Figure 3 – Computational grid used in the simulations

Boundary conditions and fluid properties were chosen to represent the real operating conditions A mass flow boundary condition was considered at domain inlets and a constant pressure condition at outlets

Figure 4 shows schematically the boundary conditions set up in the model. Mass flow was prescribed at inlets and average pressure conditions at outlets.

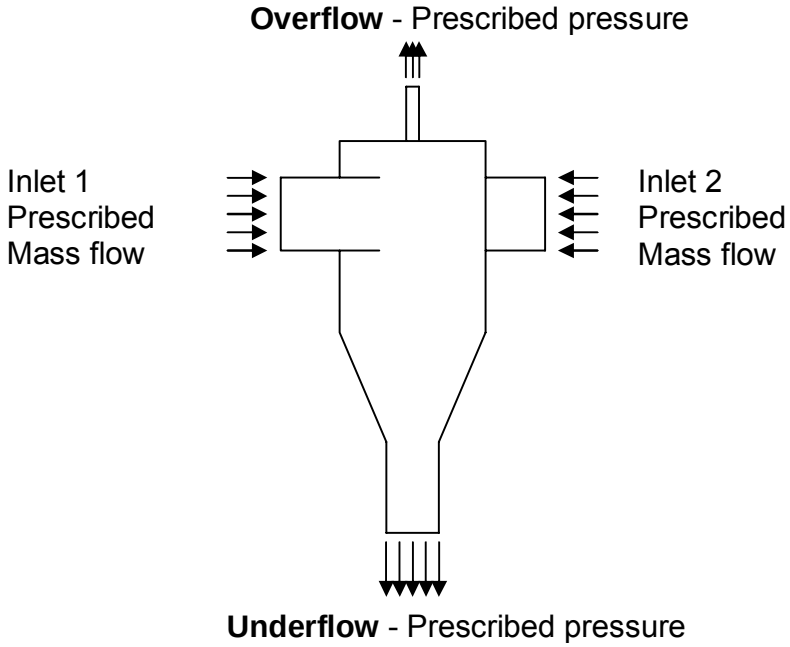

Figure 4 – Boundary conditions (scheme out of scale)

Scalable wall functions were used for the RSM for the near wall flow modeling (see CFX 5 Manual for details).

A High Resolution scheme was used as interpolation function for the advection terms. This scheme provides a second order interpolation function in all points except those regions where high gradients could lead to numerical oscillations. Then more diffusive schemes are set automatically in those regions.

Results

This section presents the results obtained with models described in previous sections. Firstly the transient results showing the dynamic behavior of the hydrocyclone will be presented, and then the results of the Algebraic Slip Model and efficiency calculations will be presented.

Transient model

A valve closing at overflow region was imposed as shown in Figure 1. For this condition, the pressure behavior overflow is shown in Figure 5. It can be seen that pressure at overflow region stabilizes within a period minor than 0.03 seconds. This rapid stabilization of flow conditions is also seen at inlet regions, as showed in Figure 6.

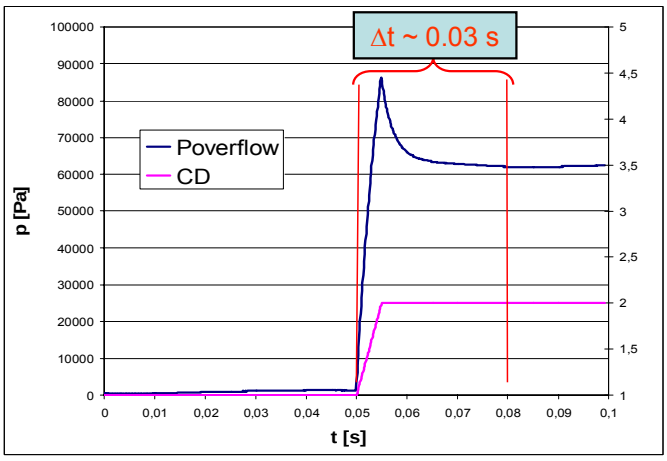

Figure 5 – Average pressure at overflow

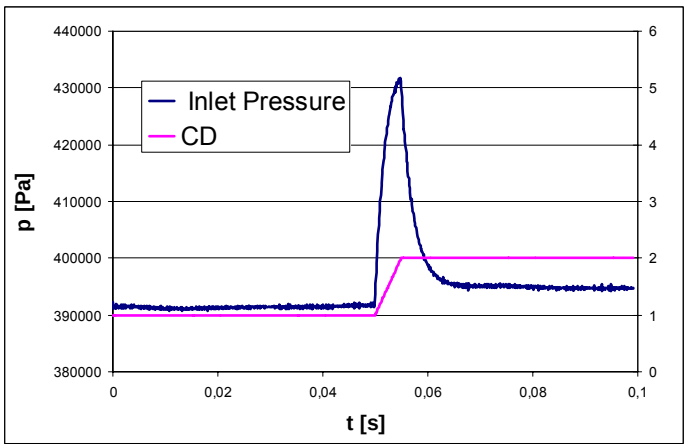

Figure 6 – Average pressure at inlets

The main conclusion from the transient model is that the new steady state is reached in approximately 0.03 seconds. This time is very small when compared with the characteristics times of the control system (for instance, the time necessary for the total closing of a valve is about 2 seconds), and so, for the purpose of control loop implementation, the dynamic behavior of the hydrocyclone could be considered as a sequence of steady states.

Efficiency calculation

The Algebraic Slip Model, described in previous sections (see Figure 2), was used to compute the hydrocyclone efficiency, considering the oil droplets as divided in six pseudo-phases or “groups” where each group represents droplets of a pre-determined diameter range.

Figure 7 and Figure 8 show the volumetric fraction on vertical planes, for the droplets groups of 0.635μm, 13.82 μm and 156.5μm. These diameters correspond to group sizes 1, 4 and 6, respectively. Figure 9 shows the total oil volume fraction distribution on vertical planes (red, represents higher fractions).

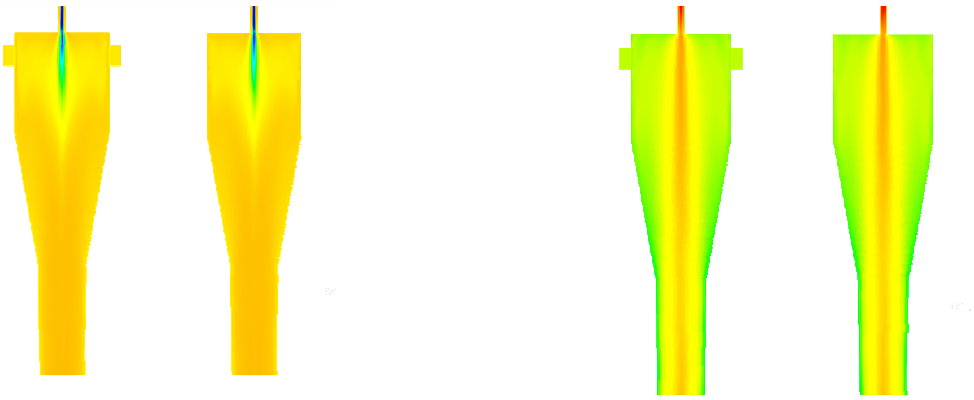

Figure 7 – Group 1 (d=0.635 μm) and 3 (d=13.82 μm) oil volume fraction distribution

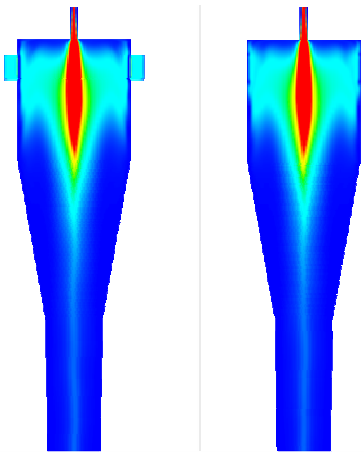

Figure 8 – Group 6 (d= 156.4 μm) oil volume fraction distribution

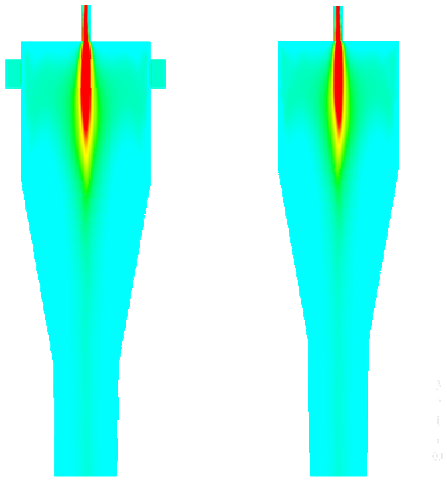

Figure 9 – Total oil volume fraction distribution

It could be observed that, for the smaller groups a considerable oil fraction is carried out to the underflow. This is because the minor droplets are dragged to the underflow as the greater ones are separated. It was also observed that the cut diameter corresponds just to the droplets considered in the group 6 (d=156.5 μm). This situation leads to global separation efficiency values of about 35 %.

	Feed (Size Group Vol. Frac.)	% of oil volume	OverFlow (Size Group Vol. Frac.)	UnderFlow (Size Group Vol. Frac.)	Separation Eficiency	Mean diameter (μm)
Group 1	0,000113288	6,36%	0,000013932	0,000099356	0,122978603	0,635401
Group 2	0,00022408	12,57%	0,000027607	0,00019648	0,123201535	1,643076
Group 3	0,00027094	15,20%	0,000033989	0,00023695	0,125448439	5,129198
Group 4	0,00061384	34,45%	0,00008683	0,00052704	0,141453799	13,82724
Group 5	0,000132534	7,44%	0,000029004	0,00010356	0,218841958	30,72309
Group 6	0,0004273	23,98%	0,0004271	4,5039E-06	0,999531945	156,4894

Table 1 – Hydrocyclone separation efficiency by droplet diameter

Figure 10 depicts the separation efficiency distributed by droplet diameter. It could be seen that, for the first five groups, the separation efficiency is below 20 %. In addition, as observed in Figure 2, a considerable oil volume fraction is enclosed in the first mode of the distribution curve, i.e., included in the small size droplets group, which are dragged by the water. So, although the separation efficiency for the large droplets was 100%, the global calculated efficiency was about 35%.

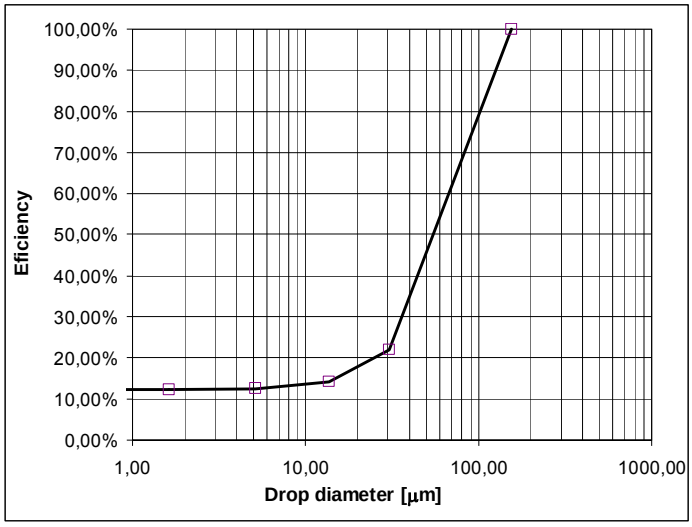

Figure 10 – Separation efficiency by drop diameter

Figure 11 shows the measured drop size distribution at the underflow. In order to compare with the simulation results, once again the droplets size groups were redistributed into six groups, as showed on the right.

Figure 12 shows the comparison of the size distribution obtained with the computational model and the measured distribution at overflow stream, already redistributed in six size groups.

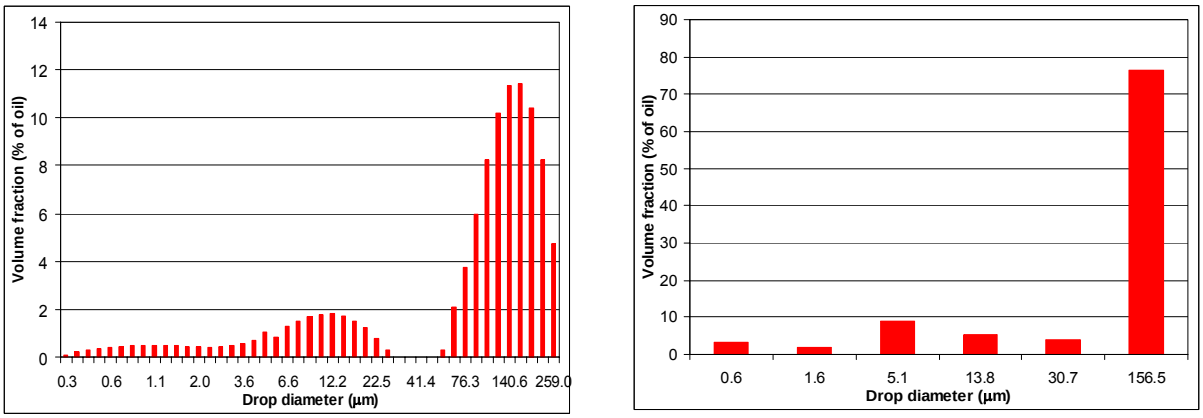

Figure 11 – Measured distribution at inlets and Overflow and representation used in simulations

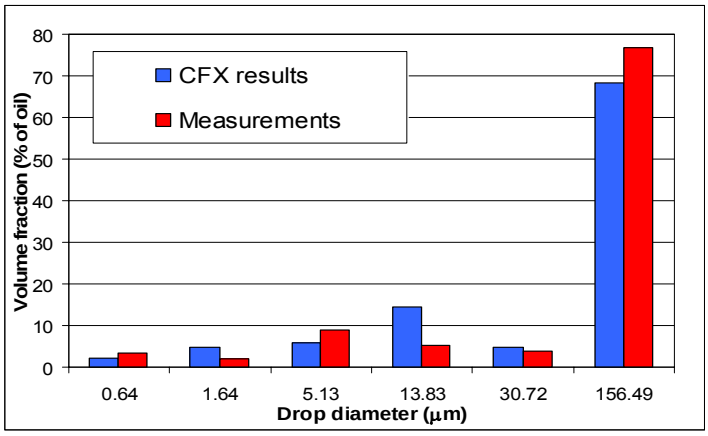

Figure 12 – Comparison of measured size distribution at overflow and CFX results

The size distribution at overflow indicates that mainly droplets of size group 6 (d=156 μm) were carried to the overflow and a minor fraction of other sizes. It could be observed good agreement between calculated and measured distribution.

Conclusions

A CFD model was implemented in order to analyze the transient hydrodynamic behavior of a hydrocyclone and predict its separation efficiency.

For the transient analysis, the effects of a valve closing were simulated. This resulted in a severe change in the device operational condition. Nevertheless, it was seen that fluid dynamic variables stabilize in a period of time of about 0.03 seconds. Mass flow at overflow and underflow usually take more time to stabilize but the pressure field stabilizes rapidly due to fluid incompressibility. In all cases the required time to reach steady state after the perturbation is very small when compared with the control system characteristic times of about 2s (time taken for a valve to open or close).

As expected, the separation efficiency is strongly dependent on the drop diameter. The calculated separation efficiency was low when compared with values commonly encountered in these devices. This could be mainly attributed to the fact that a large fraction of oil is divided in small droplets as almost 70% in volume is enclosed in the first mode of the size distribution curve. For the sizes representing the first mode, the separation efficiency is below 20%, which results in a low overall efficiency. In addition, some oil droplets coalescence could take place, not considered in the model. Investigations are being carried out in this direction, and also in modeling hydrocyclones operating with larger oil concentrations.

Acknowledgements

This work was done with financial support of PETROBRAS S.A. First author would like to thank ESSS – Engineering Simulation and Scientific Software for the financial support to attend this meeting.

Nomenclature

$\mathbf{U}$	Bulk velocity vector
$\mathbf{u}$	Dispersed phases velocity vector
ρ	Bulk fluid mass density
$\rho\overline{u_i u_j}$	Turbulent stress tensor component
ε	Turbulent kinetic energy dissipation rate
$\mathbf{T}, \mathbf{T}_C^{Turb}$	Viscous and turbulent stress tensors
C_{S1}, C_{S2}, C_{r1}, C_{r2}, C_{r3}, C_{r4}, C_{r5}	Reynolds Stress Model constants
P_{ij}	Turbulent kinetic energy production
C_D	Interphase drag coefficient
d_P	Droplet diameter

References

1. Ishii, M., One-dimensional drift-flux model and constitutive equations for relative motion between phases in various two-phase flow regimes. Vol. 77, pp 47, 1977.
2. Manninen, M. and Tavassalo, V., On the Mixture Models for Multiphase Flow. 1996.
3. Speziale, C. G., Sarkar, S., Gatski, T. B., (1991), Modelling the pressure-strain correlation of turbulence: an invariant dynamical systems approach, Journal Fluid Mechanics, Vol. 277, pp 245-272.
4. Launder, B. E., Reece, G. J., Rodi, W., (1975), Progress in the developments of a Reynolds-stress turbulence closure, Journal of Fluid Mechanics, Vol. 68, pp 537-566.